Journal of Ceramic Processing Research. Vol. 17, No. 7, pp. 659~665 (2016)

J O U R N A L O F
Ceramic Processing Research

Synthesis of the Mn^{4+}-doped $MgO-MgF_2-GeO_2$ phosphor systems for LED application

Yong Ha Choi, Myoung Su Jang and Jae Soo Yoo*
School of Chemical Engineering and Materials Science, Chung-Ang University, Seoul 06974, Korea

A rare-earth free red-emitting $MgO-MgF_2-GeO_2 : Mn^{4+}$ phosphors were synthesized and optimized for maximal luminescent intensity by the solid-state reaction. The excitation spectrum consists of two broad bands due to the Mn^{4+} ion, covering the wavelength range from 250~480 nm. The main peak of the excitation band is located at 420 nm. It provides pure red light, which is of 658 nm wavelength with narrow full-width at half-maximum of 15 nm upon 420 nm excitation. The luminescence intensity of $3.5\,MgO{\cdot}0.5MgF_2{\cdot}GeO_2 : Mn^{4+}$ could be enhanced by choosing proper flux of SrF_2, in particular. The $3.5\,MgO{\cdot}0.5MgF_2{\cdot}GeO_2 : Mn^{4+}$ exhibits the Commission International de I'Eclairage (CIE) chromaticity coordinates of (0.7154, 0.2846). The white LED was fabricated by blending two phosphors of $3.5\,MgO{\cdot}0.5MgF_2{\cdot}GeO_2 : Mn^{4+}$ and β-SiAlON : Eu^{2+} (green emitting phosphor) on the 420 nm emitting UV-chip as well as 450 nm emitting blue chip. Usual Color Rendering Index (CRI), i.e., the mean value of CRIs from R1 to R8, is 84.9 and its color gamut could be extended by 126.4%, comparing to sRGB.

Key words: Phosphor, LED, Mn^{4+}, FWHM.

Introduction

The white light-emitting diodes (WLEDs) have become the popular lighting source for car application as well as LCD backlighting. Besides, their application is expanding to medical sector due to the color flexibility. First of all, the most favorable features of this solid state lighting are high efficiency, eco-friendliness and longevity [1-8]. The most general implementation method of a WLED is to combine InGaN blue emitting chip with $YAG : Ce^{3+}$ yellow phosphor and organic silicon [9-10]. It has high Correlated Color Temperature (CCT), while the Color Rendering Index (CRI) is relatively low due to the absence of red component. Therefore, the red phosphor which has proper emission characteristics is required to achieve high color rendering. There are two ways to solve this problem. First, using three types of Blue, Green and Red LED chip. This approach may emit good light, but has disadvantage of high manufacturing and operating cost [11-13]. The other way, which is now the most popular, is to combine two or more kinds of proper phosphors for producing white light. For example, a good quality of white light can be produced with green-emitting and red-emitting phosphor on blue LED. This method implements very economical approach for relatively high quality of white light. The continuous research has been proceeded and the requirements of the green-emitting and red-emitting phosphors for WLED application are well proposed [14-15]. Meanwhile, many kinds of red phosphors were developed by several researchers. As representative red phosphors is $CaAlSiN_3 : Eu^{2+}$ (CASN) which uses Eu^{2+} as activator. This phosphor is commonly used in LED for superior properties [16-18]. In general, nitride compound can be synthesized at high temperature and high pressure. The synthetic route of CASN phosphor is very difficult. It can be synthesized at gas pressure sintering furnace. The operating condition is above 1800 °C at 0.5 MPa. Besides, the wide range of absorption band of CASN phosphor causes reabsorption when it is combined with green phosphor, which leads efficiency decrease [19-20].

The other red-emitting phosphor is $3.5\,MgO \cdot 0.5\,MgF_2 \cdot GeO_2 : Mn^{4+}$ (MGF) which was reported in 1950s. This phosphor does not uses rare earth metal. It uses Mn^{4+} as activator, which is abundant in the earth. The MGF Phosphor excites at near-UV and blue light region, and emits deep red light at 658 nm, which has narrow full width at half maximum (FWHM) of 15 nm [21-24]. The advantage of using narrow-band red phosphor such as MGF is able to have high CRI and R9 value. Also, it may widen the color gamut [25-27]. The MGF phosphor is excited by near-UV or blue light and exhibit red emission at 620-700 nm, which are assigned to the $^4A_2 \rightarrow {}^4T_2$ and $^2E \rightarrow {}^4A_2$ transitions of Mn^{4+}, respectively. Since the $^4A_2 \rightarrow {}^4T_2$ transition is spin-allowed, the excitation band is broad near visible range. While, the spin-forbidden $^2E \rightarrow {}^4A_2$ transitions is dependent on the Mn^{4+}-ligand covalency in octahedral site and emission spectrum is very narrow, which is

*Corresponding author:
Tel : +82-2-820-5274
E-mail: jsyoo@cau.ac.kr

quite different from that of the CASN. Obviously, the emission and the excitation characteristics of Mn^{4+}-activated phosphors are pretty adequate for the WLEDs application in terms of energy efficacy as well as color rendering index [28-31].

The purpose of this work is to check the feasibility of $MgO\text{-}MgF_2\text{-}GeO_2 : Mn^{4+}$ phosphor system to the WLEDs application. We study the effects of the various fluxes on luminescent characteristic of phosphors and try to optimize the synthetic route of the $MgO\text{-}MgF_2\text{-}GeO_2 : Mn^{4+}$ phosphor. Then, the WLEDs were fabricated through the coating of the synthetic phosphors and $\beta\text{-}SiAlOn : Eu^{2+}$ on the InGaN UV chips ($\lambda_{em} = 420$, 450 nm). The optical characteristic of the WLEDs are analyzed in terms of the luminous flux and color gamut. The White LED was fabricated by blending two phosphors MGF and $\beta\text{-}SiAlON : Eu^{2+}$ (green emitting phosphor) on the 420 nm emitting UV-chip as well as 450 nm emitting blue chip.

Experimental

A series of Mn^{4+}-activated phosphor system was synthesized by the solid-state reaction at high temperature. The sold-state reaction is efficient method to synthesize a phosphor. It is the most common synthetic route for commercial phosphor. The solid state reaction at high temperature typically includes pre-treatment and post-treatment. In pre-treatment step, the raw material should be done washing and drying to remove impurities. The starting materials for synthesizing the $MgO\text{-}MgF_2\text{-}GeO_2 : Mn^{4+}$ were MgO, MgF_2, GeO_2 and $MnCO_3$ (99.9%,. The alkaline fluoride materials, which are considered as flux of reacting agents, are MgF_2, CaF_2, SrF_2, BaF_2, NH_4F, NaF, and AlF_3. These materials were supplied by Kohundo Co. and their purity are all 99/99.9%. The starting materials were mixed at a desired stoichiometric ratio and ball-milled with IPA (isopropyl alcohol) at room temperature. The mixtures were pre-fired at 800 ºC in atmosphere environment for 6 hrs in a tube furnace. The pre-fired product was crushed and then milled thoroughly before the final firing, which is optimized for maximal PL intensity. After post heat-treatment, phosphor samples were cleaned by acid for removing the reactant residue, including flux material.

The prepared phosphor was analyzed with Powder X-ray diffraction (Bruker, D8 Advance, Germany) at wavelength of Cu K radiation ($\lambda = 1.540562$) to identify their phase and crystal structure. We also examined the sample using scanning field emission-scanning electron microscope (FE-SEM, Zeiss, Germany) to investigate the particle size and morphology. The room temperature photo-luminescent emission (PL) and excitation (PLE) spectra were recorded using a Xenon lamp (PSI, Korea).

Phosphor-converted white LEDs were fabricated by coating two phosphors of $MgO\text{-}MgF_2\text{-}GeO_2 : Mn^{4+}$ and $\beta\text{-}SiAlON : Eu^{2+}$ (green emitting phosphor) on the 420 nm and 450 nm emitting UV-chip. The mixing ratio of green phosphor and red phosphor are 15 : 85 and 20 : 80 in weight percent, respectively. And mixing ratio of total phosphor and silicone resin is 3 : 10 in weight percent.

Results and Discussion

The crystal structure of matrix is crucial to the influence on luminescence. Any change may cause the matrix absorption so that the transmission process of energy can be changed. In the process of compositing fluorescent powder, the raw material ratio decides the composition of products, and even tiny changes can influence the luminescent properties of products such as luminous efficiency and luminescent spectrum, including chromaticity coordinate. Not only one kind of element content has the influence, the content ratio between elements can also have influence correspondingly. In the experiment, a large number of experiments are repeated to confirm the ratio of raw materials. This is aimed at getting excellent fluorescent powder. In the experiment, pretreated powder mixtures were loaded into the high-temperature furnace, and samples were obtained through the different

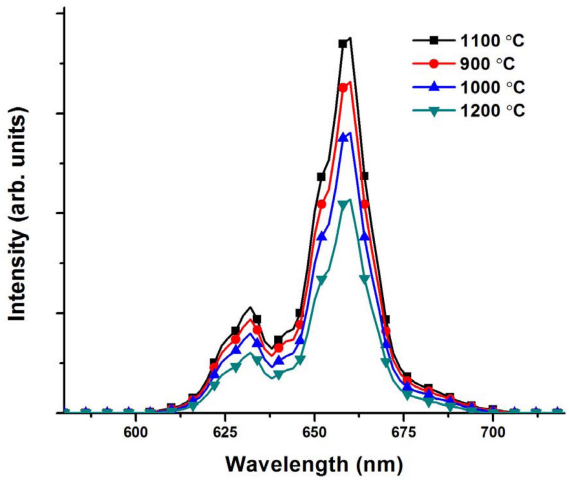

Fig. 1. Emission spectra ($\lambda_{ex} = 420$ nm) of MGF Phosphor at different temperatures synthesis.

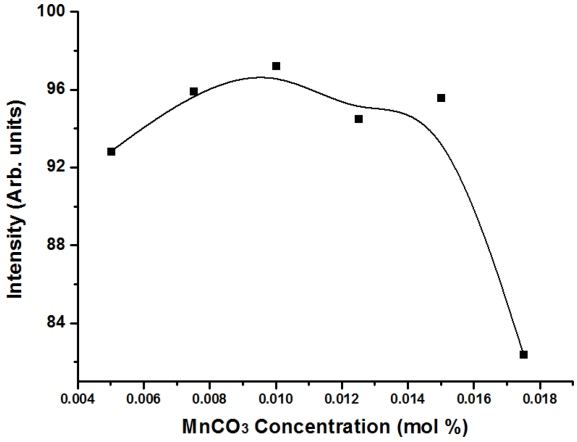

Fig. 2. Emission spectra ($\lambda_{ex} = 420$ nm)of MGF with different $MnCO_3$ concentration.

calcination temperatures. The emission spectrum of powder that was calcined at different temperatures are shown in Fig. 1. With the rise of calcination temperature, the luminescent intensity of samples grows gradually. When the calcination temperature reaches to 1100 °C, the luminescent intensity of the sample is the strongest, but it goes down when it is calcined continuously above 1200 °C. So, in the first heat-treatment experiment, the optimum firing temperature was set at 1100 °C.

Fig. 2 shows the dependence of the luminescence intensity of MGF on the contents of Mn^{4+}, which replacing the germanium ions in host matrix. The phosphor luminescence intensity is increasing with the Mn^{4+} concentration when excited at 418 nm. The highest emission intensity was observed around x = 0.01 and then, the concentration quenching of MGF was shown.

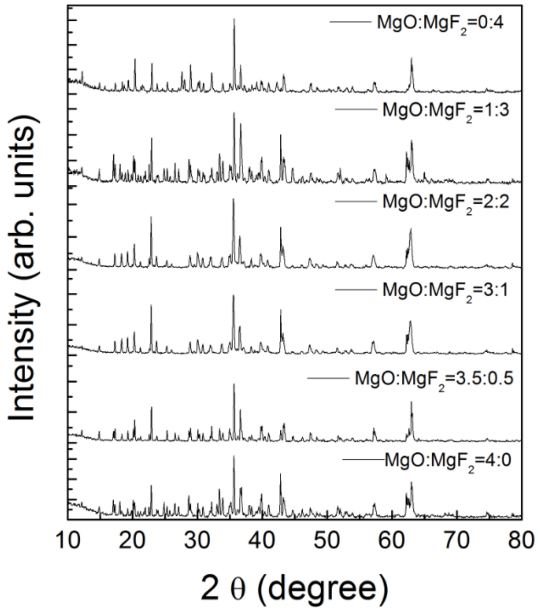

Fig. 3. The XRD diffraction pattern of various phases with ratio of starting materials MgO-MgF_2.

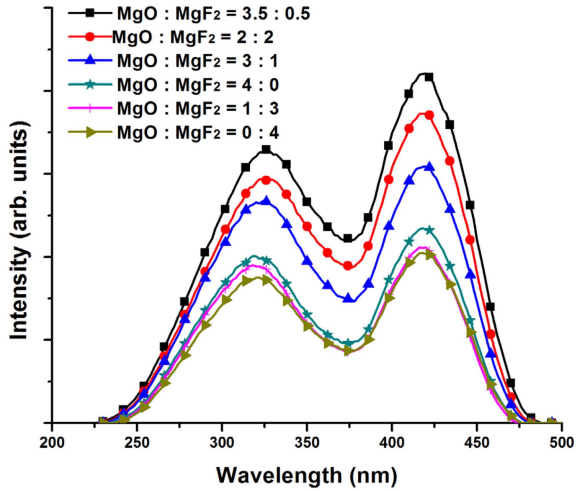

Fig. 4. Excitation spectra of MGF with ratio MgO to MgF_2.

Concentration quenching is mainly caused by energy transfer among Mn^{4+} ions. When the concentration of Mn^{4+} ions increased, the probability of energy transfer from one Mn^{4+} ion to another Mn^{4+} ion was increased as the distance between them was decreased. Since the from ^2E-$^4A_2$ transition of Mn^{4+} ions is allowed and the luminescence spectrum overlaps, non-radiative energy transfer among Mn^{4+} ions occurred as result of an electric multipolar interaction and radiation re-absorption. Furthermore, the overlap of the emission and excitation spectra indicates that the interaction caused energy migration, indicting another factor promoting concentration quenching.

For getting to the best luminescent material, the X-ray diffraction patterns of the phosphors were examined by varying the mole ratios of starting materials. By using MgO, MgF_2 and GeO_2 as starting materials, several phosphor samples were synthesized at 1100 °C for 6 hr. Fixing 0.5 mole of GeO_2 and 0.005 mole of Mn element, only mole ratio of MgO by MgF_2 is varied between 4 : 0 and 0 : 4. As shown in Fig. 3, at ratio 4 : 0 the phosphors are not well-crystallized as very low intensity was observed in the XRD pattern. Increasing mole fraction of MgF_2, several other structures (i.e., $Mg_{28}Ge_{10}O_{48}$) start to be formed and unreacted impurity (MgO) also remains at 4 : 0 ratio. At ratio of 1 : 3 $Mg_{28}Ge_{10}O_{48}$ and 3.5MgO-0.5MgF_2-0.5GeO_2 are co-existed, which is newly formed. Further analysis of the XRD patterns, one can

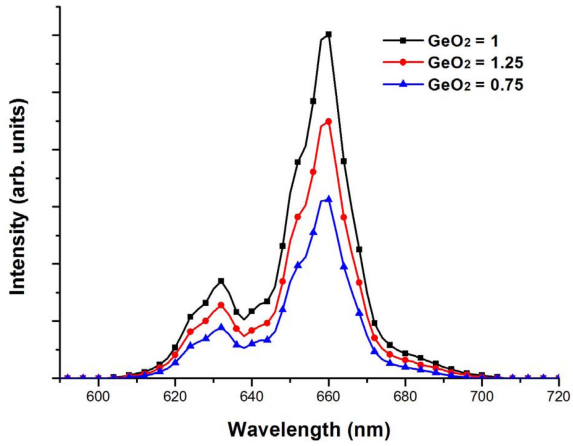

Fig. 5. Emission spectra (λ_{ex} = 420 nm) of MGF with different GeO2 concentration.

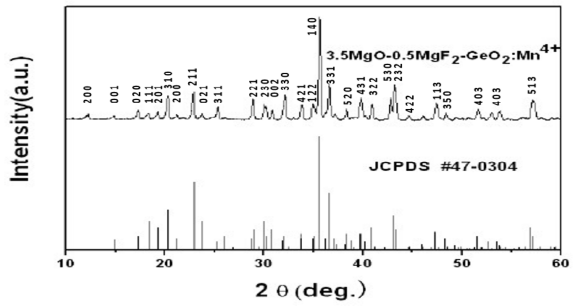

Fig. 6. The XRD diffraction pattern of MGF.

find that the diffraction pattern forms well with MgF_2. However, when the MgO adding amount more than 0.5mol, unknown phase appears. When the ratio of MgO and MgF_2 is 3.5 : 0.5, the single-phase is formed and no intermediate/impurity phases is not observed. With this ratio, absorption intensity is the most efficient, as shown in Fig. 4. The excitation intensity is the strongest in $3.5\,MgO{\cdot}0.5MgF_2{\cdot}0.5GeO_2$ composition. In the previous experiments, for study the best stoichiometric ratio relationship between MgO-MgF_2, stoichiometric number of GeO_2 was fixed to 0.5. But, that value was also adjusted for maximal luminescent intensity. The influence of different amount of GeO_2 in host matrix on emission spectrum is shown in Fig. 5. Luminous intensity increases with the total amount of GeO_2 and is maximized at the 1 mole fraction of GeO_2. Adding more GeO_2 makes the intensity be decreased. The Optimum composition could be found at $3.5MgO{\cdot}0.5MgF_2{\cdot}\ GeO_2{:}Mn^{4+}$. Fig. 6 is the XRD chromatogram of the MGF phosphor powder. The major diffraction peak is almost consistent with that of standard card (JCPDS#47-0304), which is orthorhombic system. As of our knowledge, the exact crystal structure with this composition remains unclear. But, we believe that single crystals of magnesium fluorogermanate have been grown from a melt composition of $3.5\,MgO{\cdot}0.5MgF_2{\cdot}\ GeO_2{:}Mn^{4+}$, in fluoride-based flux. The crystals are isomorphous with magnesium germanate, $Mg_{28}Ge_{10}O_{48}$. The space group is Pbam and a = 14.343(l), b = 10.196(l), and c = 5.9075(4), as depicted in Fig. 7. Typical SEM images of the Mn^{4+}-doped MGF red phosphor powder synthesized at initial process condition at 1100 °C for 6 hrs are presented in Fig. 8. The red-emitting MGF phosphor had larger diameters (15 ~ 30 μm in diameter) with plate texture.

Here again, more study on the flux had been done for complete reaction through ion transport. Conducting this experiment was based on the enhancement of luminescence intensity. However, it can influence the morphology and powder status such as shrinkage of the final phosphor, as well. PL spectra of MGF phosphors which content various fluoride materials are shown in Fig. 9. MGF phosphors emits very sharp and deep red light. As one can see, MGF phosphor has sharp luminescence peak that has 15 nm of FWHM at the peak wavelength of 658 nm. PL intensity of the phosphor may be improved by alkaline fluoride materials. We tried following materials: SrF_2, NH_4F, CaF_2, NaF, BaF_2, MgF_2, and AlF_3. The sample with SrF_2 shows the highest PL intensity among them. Figure 10 shows the emission

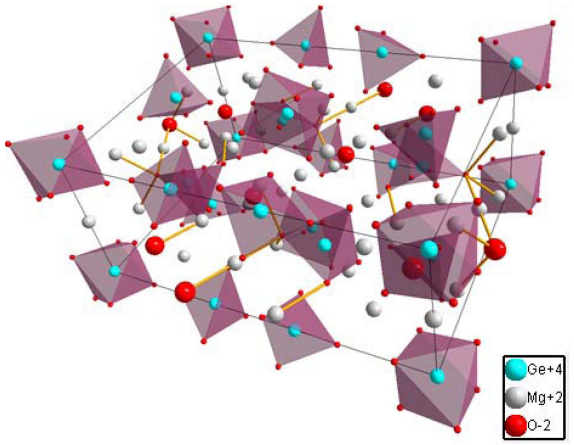

Fig. 7. Crystal structure of MGF.

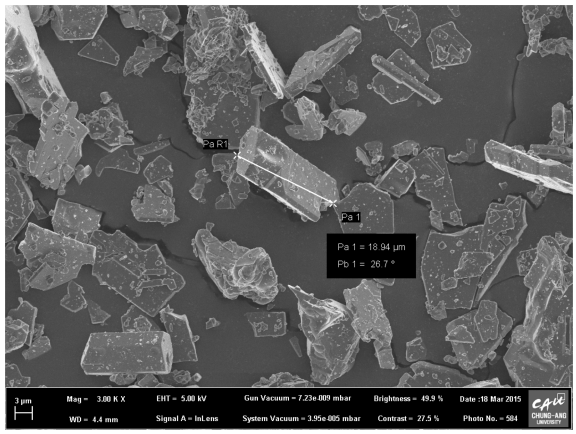

Fig. 8. SEM Image of MGF phosphors.

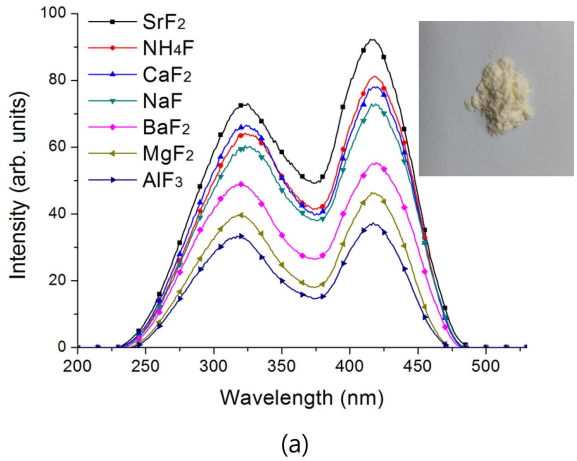

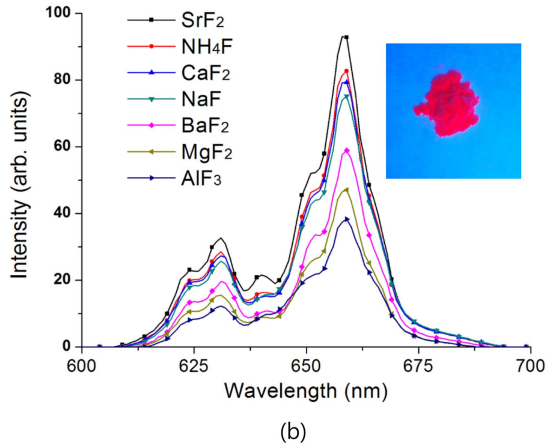

Fig. 9. (a) Emission spectra (λ_{ex} = 420 nm)of MGF with different flux (b) Excitation spectra (λ_{em} = 658 nm) of MGF with different flux.

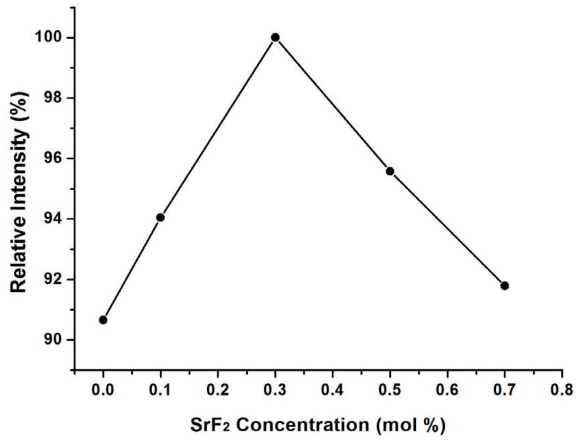

Fig. 10. Emission spectra (λ_{ex} = 420 nm) of MGF with different SrF_2 concentration.

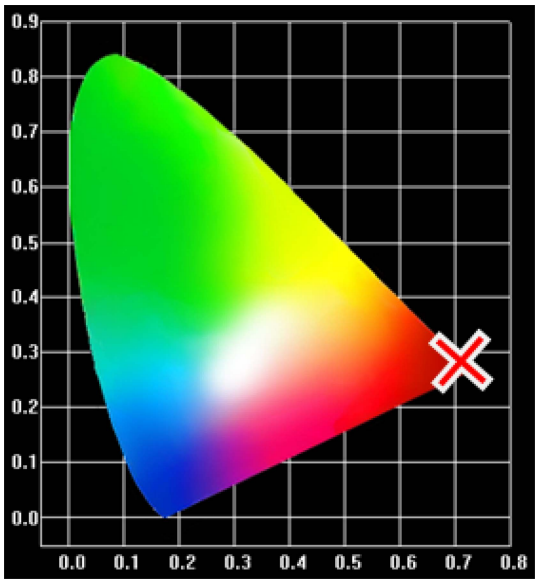

Fig. 11. CIE chromaticity coordinates of MGF phosphors.

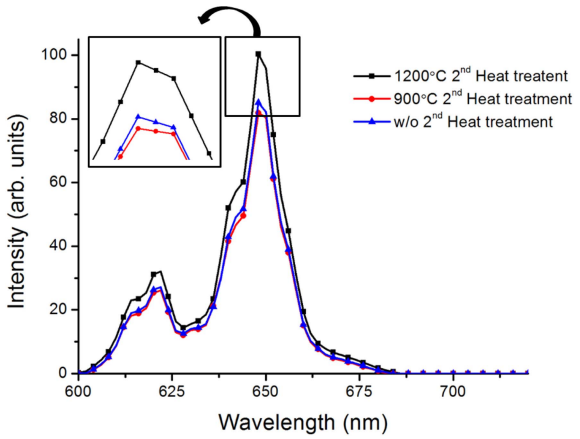

Fig. 12. Emission spectra (λ_{ex} = 420 nm) compare pre-heat treatment with sec-heat treatment.

spectra of MGF phosphor when using different amounts of SrF_2. It shows the dependence of the luminescence intensity of MGF on the concentration of

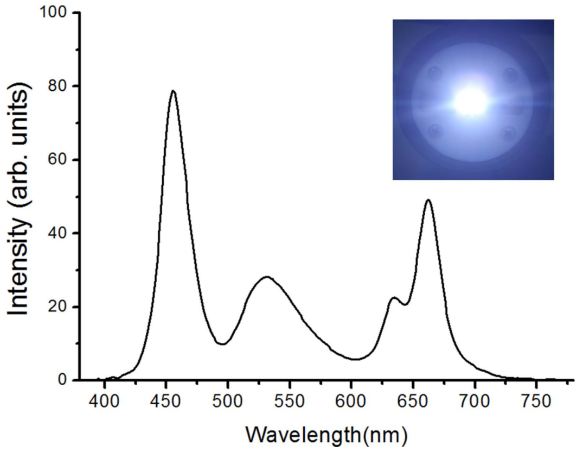

Fig. 13. Packaged WLED emission spectrum with blue LED chip (450 nm), MGF phosphors and β-SiAlOn : Eu^{2+}.

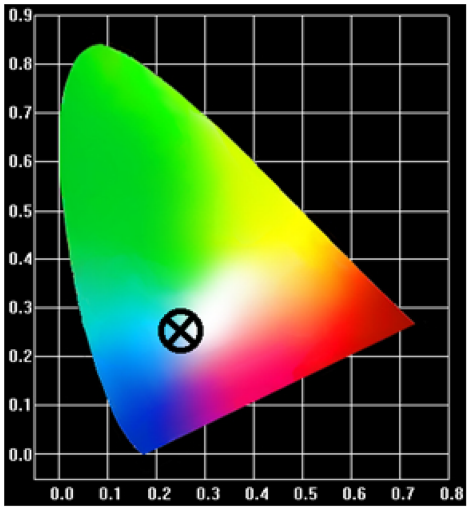

(a)

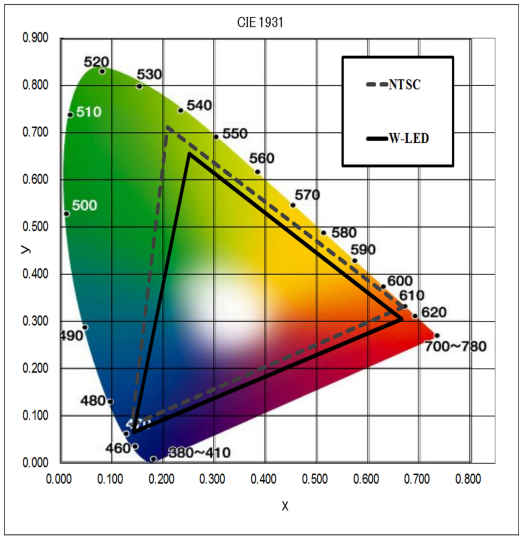

(b)

Fig. 14. Color coordinate and color gamut of packaged WLED with blue LED chip (450 nm), MGF phosphors and β-SiAlOn : Eu^{2+}.

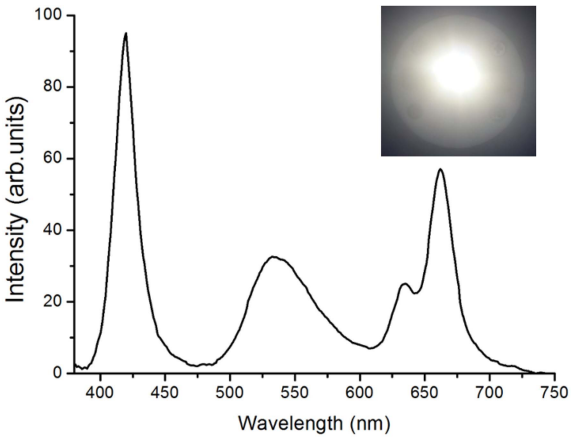

Fig. 15. Packaged WLED emission spectrum with blue LED chip (420 nm), MGF phosphors and β-SiAlON : Eu^{2+}.

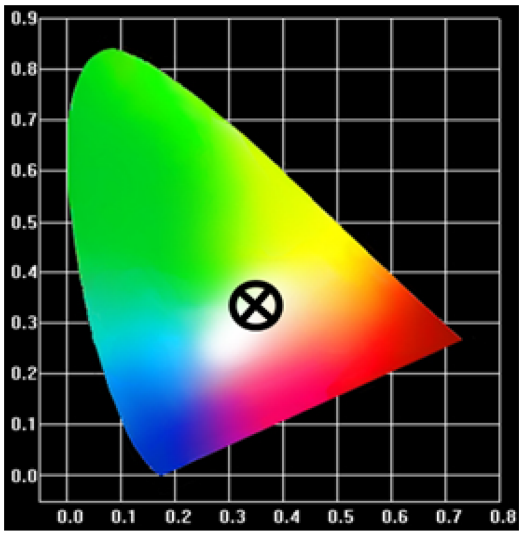

(a)

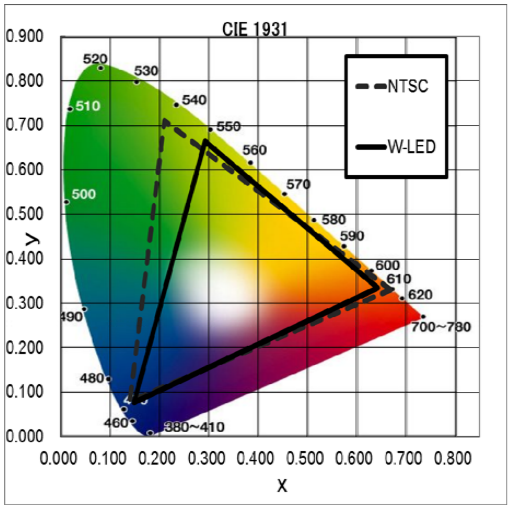

(b)

Fig. 16. Color coordinate and color gamut of packaged WLED with blue LED chip (420 nm), MGF phosphors and β-SiAlON : Eu^{2+}.

flux. We do not find any change in XRD pattern in this results and found that the SrF_2 is used as a typical flux material. Obviously, too much contents of SrF_2 makes luminescence intensity be decreasing. As shown in Fig. 11, CIE chromaticity color coordinate of MGF phosphor are fixed at (0.7154, 0.2846). This result shows that flux materials do not have any influence on color chromaticity of phosphor, as expected.

In most of the phosphor synthesis experiments, in order to improve the luminous efficiency of the phosphor, the additional heat-treatment is usually carried out. The red-emitting MGF phosphor after full optimizing process was tried to do second heat-treatment in this experiment. As shown in Fig. 12, luminescence was improved by second heat-treatment. When the second heat-treatment time rising more than 10 hours, phosphor MGF luminous efficiency is maximized. But, it has no change with increasing heat-treatment time for more than 20 hours.

Fig. 13 shows packaged WLED emission spectrum with blue LED chip (450 nm), MGF phosphors and â–SiAlON : Eu^{2+}. It has 84.9 of CRI value and its CIE chromaticity color coordinate is (0.2607, 0.2821) as shown in Fig. 14. And this WLED package has large color gamut. It has 89.5% area ratio comparing with NTSC color gamut. And it is 126.4% area ratio comparing with SRGB color gamut and its luminous flux is 8.11 lm. Fig. 15 shows packaged WLED emission spectrum with blue LED chip (420 nm), MGF phosphors and β-SiAlON : Eu^{2+}. It has 58.6 of CRI value and its CIE chromaticity color coordinate is (0.3496, 0.3340) as shown in Fig. 16. And this WLED package has large color gamut. It has 84.5% area ratio comparing with NTSC color gamut. And it is 119.4% area ratio comparing with SRGB color gamut and its luminous flux is 7.57 lm. These data show that MGF phosphors are promising for use in WLED.

Conclusions

The $3.5MgO{\cdot}0.5MgF_2{\cdot}GeO_2{\cdot}:Mn^{4+}$ phosphor was synthesized by conventional soloid-state method. This phosphor shows good photoluminescence property at 658nm (λ_{ex} = 420 nm). When some fluoride materials are added by flux, photoluminescence property is increased. Particularly, SrF_2 was the most efficient in our experimental regime. The WLED is fabricated by integrating blend phosphors of MGF and β-SiAlON : Eu^{2+} on the 420 nm and 450 nm emitting UV-chip. They have 58.6 and 84.9 of CRI value respectively. And their CIE chromaticity color coordinate are (0.3496,0.3340) and (0.2607, 0.2821) respectively. These results indicate MGF phosphor is a promising candidate for WLEDs.

Achnowledgments

This research was supported by the Chung-Ang

University Research Scholarship Grants in 2015.

References

1. C. Wu, J. Li, H. Xu, J. Wu, J. Zhang, Z. Ci, and Y. Wang, Journal of Alloys and Compounds 646 (2015) 734-740.
2. R. Cao, M. Peng, E. Song, and J. Qiu, ECS Journal of Solid State Science and Technology 1[4] (2012) R123-R126.
3. L. Meng, L. Liang, and Y. Wen, Journal of Materials Science: Materials in Electronics 25[6] (2014) 2676-2681.
4. H.G. Kang, J.K. Park, C.H. Kim, & S.C. Choi, Journal of the Ceramic Society of Japan 117[1365] (2009) 647-649.
5. L. Wang, Y. Xu, D. Wang, R. Zhou, N. Ding, M. Shi, & Y. Wang, physica status solidi A 210[7] (2013) 1433-1437.
6. Y.H. Jin, Y.H. Hu, J. Alloys Compd. 610 (2014) 695-700.
7. Z. Chen, J.H. Zhang, S. Chen, M.Y. Lin, C.Q. He, G.D. Xu, M.M. Wang, X.F. Yu, J.Q. Zou, K. Guo J. Alloys Compd. 632 (2015) 756-759.
8. K. Kakinuma, Jpn. J. Appl. Phys. 45 (2006) 4330.
9. S. Okamoto, and H. Yamamoto, Journal of The Electrochemical Society 157[3] (2010) J59-J63.
10. P. Pust, P. J. Schmidt and W. Schnick, Nat. Mater. 14 (2015) 454.
11. J.Y. Han, W.B. Im, G.Y. Lee, and D.Y. Jeon, J. Mater. Chem. 22 (2012) 8793.
12. M.M. Shang, J. Fan, H.Z. Lian, Y. Zhang, D.L. Geng and J. Lin, Inorg. Chem. 5[4] (2014) 7748.
13. W. Lu, W.Z. Lv, Q. Zhao, M.M. Jiao, B.Q. Shao and H.P. You, Inorg. Chem. 53 (2014) 11985.
14. C.H. Huang, and T.M. Chen, Opt. Express 18[5] (2010) 5089.
15. M.S. Shur, and A. Zukauskas. Proceedings of the IEEE 93[10] (2005) 1691-1703.
16. K. Uheda, N. Hirosaki, Y. Yamamoto, A. Naito, T. Nakajima, and H. Yamamoto, Electrochem. Solid-State Lett. 9 (2006) H22.
17. R.J. Xie, N. Hirosaki, Sci. Technol. Adv. Mat. 8 (2007) 588-600.
18. R.J. Xie, N. Hirosaki, Y.Q. Li, T. Takeda, Mater. 3 (2010) 3777-3793.
19. P.F. Smet, A.B. Parmentier, & D. Poelman, Journal of the electrochemical society 158[6] (2011) R37-R54.
20. R. Cao, W. Luo, Q. Xiong, A. Liang, S. Jiang, and Y, Xu, Journal of Alloys and Compounds 648 (2015) 937-941.
21. L. Thorington, J. Opt. Soc. Am. 40 (1950) 579.
22. M.E. van Ipenburg, G. J. Dirksen, G. Blasse, Mater. Chem. Phys.39(1995) 236.
23. G. Kemeny and C.H. Hakke, J. Chem. Phys. 33 (1960) 783.
24. M. Srivastava and W.W. Beers, J. Electrochem. Soc. 143[9] (1996) L203.
25. R. J. Xie, N. Hirosaki, and T. Takeda, Applied Physics Eexpress 2[2] (2009) 022401.
26. K. Kakinuma, Japanese journal of applied physics 45[5S] (2006) 4330.
27. Ryu, J.S., Kim, S.J., Park, S.M., & Ko, J.H. Journal of Information Display, 11(2), (2010) 39-44.
28. J.W. Moon, B.G. Min, J.S. Kim, M.S. Jang, K.M. Ok, K.Y. Han, and J.S. Yoo, Optical Material Express 6[3] (2016) 782-792.
29. T.G. Kim, T. Kim, Y.S. Kim, and S.J. Im, Journal of The Electrochemical Society 157[11] (2010) J397-J400.
30. A.V. Shamshurin, N.P. Efryushina, and A.V. Repin, Inorganic materials 36[6] (2000) 629-631.
31. S.J. Lee, J. Jung, J.Y. Park, H.M. Jang, Y.R. Kim, and J.K. Park, Materials Letters 111 (2013) 108-111.